Advanced Steel Construction – Vol. 20 No. 4 (2024) 397–405
DOI:10.18057/IJASC.2024.20.4.7

NUMERICAL INVESTIGATION ON SEISMIC PERFORMANCE OF PREFABRICATED STEEL BEAM-TO-COLUMN CONNECTION WITH REPLACEABLE U-SHAPED PLATE

Xun Zhang [1], Bin Zhou [1], Jun-Dong Gao [1,*], Hui Qian [1], Lian-Zhi Song [2] and Li-Ming Cai [3]

[1] *Xun Zhang, Bin Zhou, Jundong Gao and Hui Qian, School of Civil Engineering, Zhengzhou University, Zhengzhou 450001, PR China*

[2] *Lianzhi Song, Henan Xinya Steel Structure Engineering Co., Ltd, Zhengzhou 452470, RP China*

[3] *Liming Cai, Henan Architectural Design and Research Inst. Co., Ltd., Zhengzhou 450099, PR China*

** (Corresponding author: E-mail: gaojundong@zzu.edu.cn)*

ABSTRACT

This paper presents a novel prefabricated steel beam-to-column connection with a replaceable U-shaped plate (PSCU) aimed at enhancing the seismic resilience of steel structures and enabling expedited assembly, disassembly, and post-earthquake recovery. The structural design of the PSCU is delineated, along with the articulation of seismic design objectives and methodologies. A sophisticated finite element (FE) model for PSCU is constructed utilizing solid elements, and the fidelity of this modeling paradigm is validated against documented experimental findings. Quasi-static numerical simulations are conducted for 11 connection patterns with varying U-shaped plate thickness, T-shaped plate thickness and bolt quantity. Comparative investigations into hysteresis curves, failure modes, skeleton curves, and ductility coefficients affirm the precision of the seismic design objectives and methodologies. The findings underscore a pronounced ductile failure in this connection, characterized by a discernible four-stage failure progression: elastic, slip, elastic-plastic, and plastic stages. The post-earthquake recovery method for PSCU was proposed and verified, and recommendations for the design of PSCU were put forward. This research offers a robust scientific basis for the expeditious post-earthquake functional recovery in steel frame structures.

ARTICLE HISTORY

Received: 5 March 2024
Revised: 19 September 2024
Accepted: 20 September 2024

KEYWORDS

Prefabricated steel beam-to-column connection;
Replaceable U-shaped plates;
Post-earthquake functional recovery;
Seismic performance;
Numerical investigations

1. Introduction

The prefabricated steel structure, regarded as a sustainable building with a complete lifecycle, offers advantages such as standardized production, a short construction period, flexible space layout, and substantial economic benefits. It has evolved into a pivotal structural form in developed nations such as Europe, America, and Japan [1,2]. To circumvent brittle failure at the root weld of beam-column connections and adhere to seismic design criteria emphasizing "strong column and weak beam, strong connection and weak connected members," traditional steel frame beam-column connections have historically employed two primary methods to shift the plastic hinge outward. One approach involves weakening the beam section, for example, by utilizing a dog bone section to ensure the appearance of plastic hinges at the weakened segment [3-5]. The alternative strategy is to reinforce the connection at the beam root [6,7]. However, in experimental investigations, the primary components of these connections often sustain severe damage upon connection failure, rendering conventional steel frame structures challenging to repair and restore to functional capacity post-earthquakes [8,9].

In pursuit of enhanced damage control and expeditious post-earthquake recovery for steel beam-column connections, scholars have proposed an earthquake-resilient structure [10]. This innovation aims to minimize earthquake disaster losses and reduce post-earthquake recovery time, with specific applications to beam-column connections [11-15]. However, early-stage earthquake-resilient connections introduced by scholars were generally intricate, involving cumbersome and costly replacement processes after earthquakes. Consequently, domestic scholars proposed simplified forms of connections [16,17]. For example, Zhang and Jiang et al. [18-24] devised a series of earthquake-resilient prefabricated beam-column connections, ensuring the primary structure remains in the elastic stage during earthquakes and can be restored post-earthquake by replacing the flange cover plate. In summary, earthquake-resilient beam-column connections can be effectively repaired by substituting energy-dissipating members or dampers with concentrated deformation. Nevertheless, these connections exhibit notable drawbacks. Firstly, the installation of energy-consuming components is intricate, demanding extensive disassembly and temporary support during replacement. Secondly, the larger connection area raises the complexity and cost of repair. Furthermore, other components of the connection may suffer some degree of damage, resulting in a decline in connection performance [25,26].

Addressing the limitations of existing research, this paper introduces a novel prefabricated steel beam-to-column connection with a replaceable U-shaped plate (PSCU) aimed at enhancing both seismic and post-earthquake recovery performance. The components of this connection include frame columns, H-shaped frame beams, T-shaped plates, and U-shaped plates. In comparison to traditional beam-column connections, the incorporation of the U-shaped plate in this connection enables yielding first and facilitates plastic damage control. Following an earthquake, only the U-shaped plate and high-strength bolts require replacement to achieve rapid functional recovery of PSCU. The paper delves into the theoretical design methodology, numerical simulation, and parametric analysis of PSCU, offering a dependable and cost-effective option to further realize swift assembly, high ductility, and prompt recovery of steel structures post-earthquakes.

2. Structure design and seismic design method of PSCU

2.1. Structure design for PSCU

The PSCU comprises four primary components: frame columns, frame beams, T-shaped plates, and U-shaped plates, as illustrated in Fig.1(a). Within the column, two vertical internal partitions are pre-welded at the level aligned with the T-shaped plate, ensuring even load transfer from the end of beam to the column and preventing stress concentration on the column wall. The frame beam adopts a configuration that widens the flange width at the beam end, causing the plastic hinge to manifest away from the end of beam and ensuring ample ductility for the connection. During the factory prefabrication process, two T-shaped plates are symmetrically welded on one side of the column. The U-shaped plate, fabricated from three perforated steel plates with a Q235 steel grade (lower than that of other components), undergoes yielding first and concentrates connection deformation under seismic actions. This guarantees that the main components remain free from plastic deformation. Following an earthquake, the post-earthquake recovery of this connection is easily achieved by replacing the U-shaped plate and reseting the bolt connections.

All fabrication and welding of components for this connection are executed in the factory. The contact surfaces of the bolt connections undergo sandblasting to augment the frictional energy dissipation capacity of the connection. No special treatment is applied between the frame column and the U-shaped plate or frame beam, thereby enhancing the rotational capacity and post-earthquake recovery performance of the connection. Furthermore, in comparison to other prefabricated beam-column connections, this design incorporates a finite connection area set at the root of the beam. This feature facilitates rapid recovery after an earthquake without compromising the overall structural strength.

On-site assembly involves solely bolt connections for each component, ensuring swift and efficient installation and replacement. The assembly process of PSCU is shown in Fig.1(b). The on-site assembly process of the connection can be delineated into three steps: Initially, lift the frame beam to the

predetermined position of the T-shaped plate and secure the beam to the T-shaped plate using lower flange bolts. Subsequently, place the U-shaped plate onto the upper flange of the beam and the outer side of the T-shaped plate. Sequentially connect the U-shaped plate to the beam and the U-shaped plate to the T-shaped plate using bolts. Finally, apply pretension to all bolts.

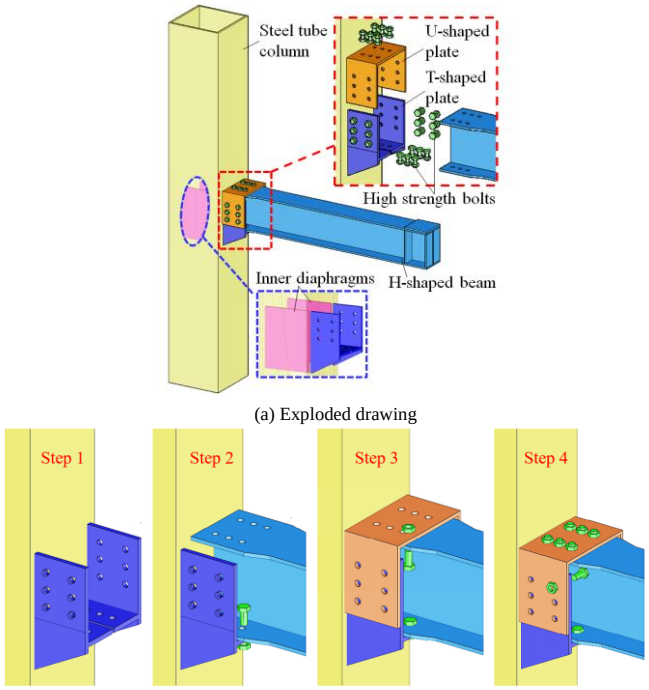

(a) Exploded drawing

(b) Assembly process diagram

Fig. 1 PSCU construction diagram

Owing to the absence of a direct connection between beams and columns in this configuration, intricate stress transmission is circumvented, and the force transmission path is illustrated in Fig.2. The vertical load (F) acted at the beam end is initially conveyed along the beam to the connecting area. As a consequence of the two bolted connections at the widened end of the beam, a part of the beam end load is successively transmitted to the U-shaped plate and T-shaped plate along the blue arrow, while the remaining load is directly transmitted to the T-shaped plate along the orange arrow. Both segments of the load traverse through the frictional force between the plates. Ultimately, the load transmitted via these two paths to the T-shaped plate is directly conveyed to the column.

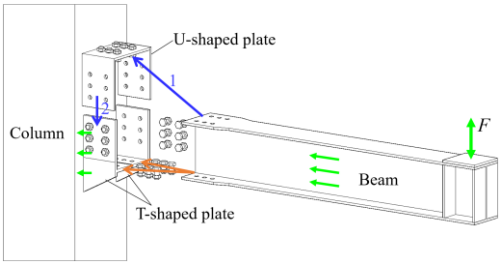

Fig. 2 Load transmission path of PSCU

2.2. Seismic design method of PSCU

The Fig.3 illustrates the connection recover measures required to achieve seismic fortification goals under different seismic actions: Under frequent earthquakes, since the connection is no slip and all components are in the elastic stage, the seismic performance of connection can be completely recovered without repair after earthquake. Under fortification earthquakes, the connection begins to dissipate energy through the friction between bolted plates and all the structural components are still in elastic stage. The seismic performance of connection can be restored by only adjusting the bolts after earthquakes. Under rare earthquakes, the U-shaped plate yields initially and the structure dissipates seismic energy through the friction between contact plates and the plastic deformation of U-shaped plates. At this moment, the performance of the connection can be restored by replacing the U-shaped plates and reseting bolts. Under extremely rare earthquakes, the flange of beam begins to yield and plastic hinge appears at the variable cross-section of beam. The seismic performance of connection can be restored by replacing the U-shaped plate, deformed beam and bolts after earthquakes. To ensure post-earthquake recovery performance of the connection, it is essential to prevent or delay the plastic deformation of T-shaped plates and columns until the latest stage.

The seismic design of PSCU is oriented towards ensuring that seismic energy is predominantly dissipated through slip between contact plates and plastic deformation of the U-shaped plate and beam. In accordance with strength calculations, section 1-1 in Fig.4 represents the section where the beam end first yields, with S_1 and S_2 denoting the connection area and the transition section of the beam, respectively.

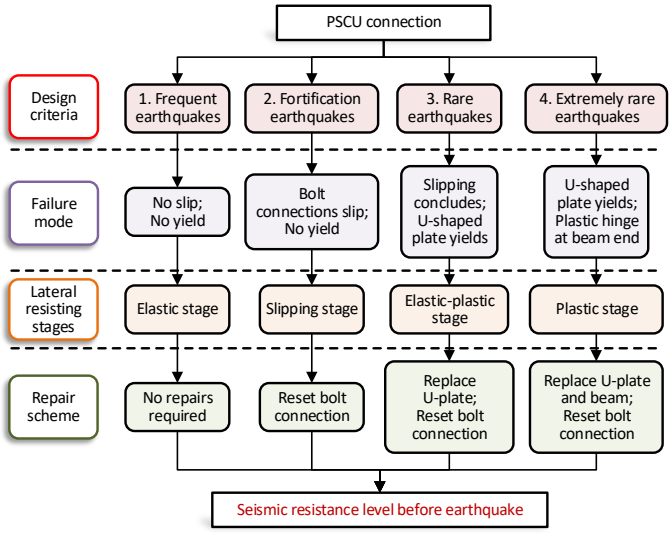

Fig. 3 Flow chart of seismic design

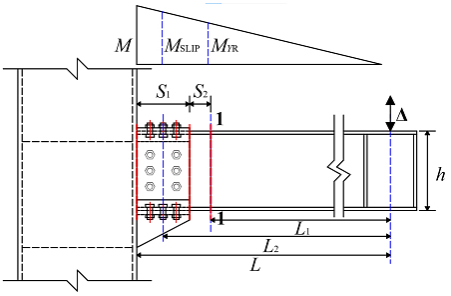

Fig. 4 Bending moment diagram of beam segment

In seismic design, the design formula for bending moment at different stages corresponds to the seismic fortification goal under various seismic actions. The PSCU should adhere to the requirements of no slip between plates during frequent earthquakes, implying that the moment satisfies Eq. (1). Under fortification earthquakes, the connection initiates slipping but does not enter the yield stage, meaning the moment satisfies Eq. (2). In the event of rare earthquakes, the bolts fully slip, the U-shaped plates yield, and the flange of the beam section 1-1 undergoes successive yielding before connection damage, signifying that the moment satisfies Eq. (3).

$$M \le M_{s,t} = \frac{L}{L_2}\left(\frac{I}{I_f} n_{bf} P \mu h\right) \tag{1}$$

$$M_{s,t} < M \le M_{y,t} = \min\left\{\frac{L}{L_2} M_{y1}, \frac{L}{L_2} M_{y2}, \frac{L}{L_1} M_{yr}\right\} \tag{2}$$

$$M_{y,t} < M \le M_{u,t} = \min\left\{\frac{L}{L_2} M_{u1}, \frac{L}{L_2} M_{u2}\right\} \tag{3}$$

Where:

M	Design bending moment value of the beam root
$M_{s,t}$	Slip bending moment value

$M_{y,t}$	Yield moment value of the beam root
$M_{u,t}$	Ultimate moment value of the beam root
L_1, L_2, L	Distances from the loading point to section 1-1, to the center of the connection area, and to the edge of the column, respectively
I, I_f	Inertia moment of the total section of the beam and the inertia moment of the beam flange, respectively
M_{yr}	Yield moment value of the beam section 1-1
n_{bf}	Number of bolts on one side of the splicing center line
P	Pre-tension of high-strength bolt
μ	Anti-slip coefficient
h	Depth of the beam

In Eq. (2), the yield load of the bolt rod M_{y1} and the yield load of the hole wall M_{y2} shall be calculated first, with the calculation methods as presented in Eq. (4) and Eq. (5), respectively. In Eq. (3), the ultimate load of the bolt rod (M_{u1}) and the ultimate load of the hole wall (M_{u2}) shall be calculated first, with the calculation methods outlined in Eq. (6) and Eq. (7), respectively.

$$M_{y1}=\frac{I}{I_f}n_{bf}h\left(0.58A_e^b f_y^{bo}+P\alpha_1\mu\right) \tag{4}$$

$$M_{y2}=\frac{I}{I_f}n_{bf}h\left(t_f D f_y^b+P\alpha_1\mu\right) \tag{5}$$

$$M_{u1}=\frac{I}{I_f}n_{bf}h\left(0.58A_e^b f_u^{bo}+P\alpha_1\mu\right) \tag{6}$$

$$M_{u2}=\frac{I}{I_f}n_{bf}h\left(t_f D f_u^b+P\alpha_1\mu\right) \tag{7}$$

Where:

A_e^b	Effective sectional area at the bolt thread
f_y^{bo}, f_u^{bo}	Yield strength and ultimate strength of bolt steel, respectively
f_y^b, f_u^b	Yield strength and ultimate strength of steel beam, respectively
α_1	Flange friction reduction coefficient
t_f	Flange thickness
D	Diameter of the screw hole

3. The establishment and validation of the FE model for PSCU

3.1. The establishment of the FE model for PSCU

Fig.5 shows the geometric details of PSCU model. The lengths of the column and beam are 3000mm and 1835mm, respectively. The steel column adopts the tube column of 400mm×350 mm×16 mm. The common section and widen flange section of H-shaped beam adopt 300mm×200mm×12mm×8mm and 300mm×250mm×12mm×8mm, respectively. All bolts are 10.9 grade high-strength bolts with a diameter of 20mm, and standard size 22mm diameter holes are provided on all components.

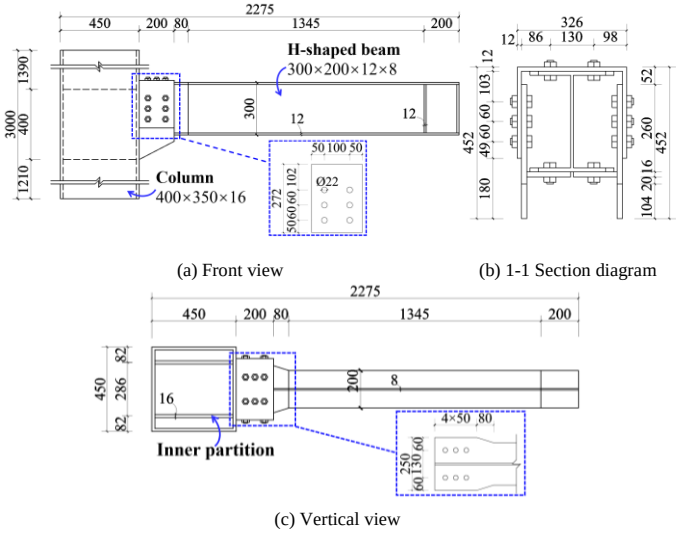

Fig. 5 Geometric dimensions of PSCU

The developed FE model of PSCU is depicted in Fig.6. The three-dimensional eight-node reduced integration solid element (C3D8R) was utilized for each component of the connection. Mesh sizes, particularly in critical areas such as bolt holes and the U-shaped plate, were refined. Contact relationships were established among the U-shaped plate, T-shaped plate, beam, and bolts. The contact property included tangential behavior with a "Penalty" friction formulation and normal behavior with "Hard Contact." The tangential friction coefficient between the contact plates was taken as 0.35, while the friction coefficients for the bolt-related contact surfaces were all set to 0.05. The material properties are shown in Table 1. The value of the ultimate strain is the strain measurement recorded when the material reaches its ultimate strength.

Table 1
Material properties of the steel and bolt

Materials	Q235	Q355	High-strength bolt
Density ρ (10^{-9}t/mm^3)	7.85	7.85	7.85
E (10^5MPa)	2.06	2.06	2.06
Poisson's ratio v	0.3	0.3	0.3
Yeild strength f_y (MPa)	235	355	940
Ultimate strength f_u (MPa)	375	470	1140
Yield strain (%)	0.145	0.184	0.470
Ultimate strain (%)	2.500	2.233	1.470

Hinge constraints were applied to the top and bottom of the column, and axial pressure with an axial pressure ratio of 0.3 was applied at one end of the column. Additionally, to prevent out-of-plane instability of the beam, lateral restraints were implemented at the free end. A rigid plate was introduced at the loading point of the beam free end to mitigate stress concentration. The positive direction was considered upward, while the opposite direction was deemed negative.

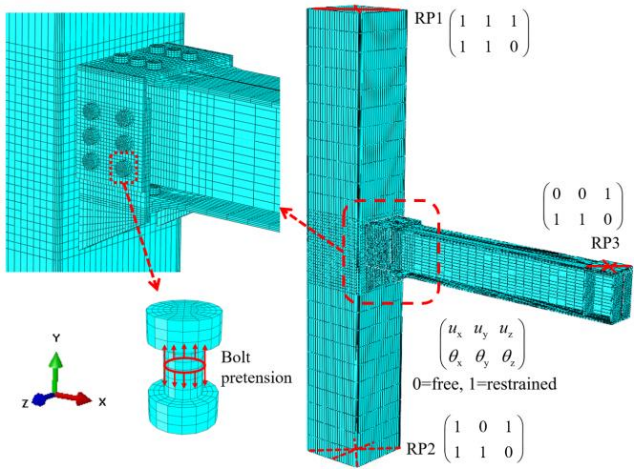

Fig. 6 FE model of PSCU

The loading process for PSCU was conducted in three sequential steps: 1) Applying pretension to the high-strength bolts; 2) Applying axial pressure at the top end of column; 3) Applying low-cycle reciprocating load at the center point of the top surface of the rigid plate. The loading system for PSCU, as per the seismic code of ANSI/AISC 341-16 [27], is illustrated in Fig.7. The cyclic displacement loading was controlled by the inter-story drift angle(θ), representing the ratio of the beam end displacement to the distance from the loading point to the centerline of column (1950mm).

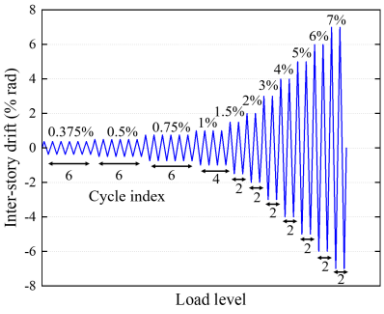

Fig. 7 Loading system

3.2. Verification of the FE model for PSCU

In order to conduct a comprehensive simulation analysis of the seismic performance and post-earthquake reparability of PSCU, it is imperative to pre-validate the established finite element model for PSCU. To achieve this, the same modeling approach employed for PSCU was utilized to model a Z-type cantilever beam splices of the column-tree connection test model (CT-SLIP) [28, 29]. The structural details of CT-SLIP are illustrated in Fig.8. A detailed comparison of the modeling parameters between PSCU and CT-SLIP is presented in Table 2.

Table 2
Model parameters of PSCU and CT-SLIP

Model	Steel tube columns				H-shaped beams				High strength bolt grade	Element type	Contact relation-ships	Friction coeffi-cient
	Length (mm)	Section size (mm)	Steel grade	Boundary	Length (mm)	Section size (mm)	Steel grade	Boundary				
PSCU	3000	200×200×16	Q355	Hinge	1950	300×200×8×12	Q235	Lateral restraints	10.9	C3D8R	Hard contact	0.35
CT-SLIP	3000	400×350×16	Q355	Hinge	1835	300×200×8×12	Q235	Lateral restraints	10.9	C3D8R	Hard contact	0.35

Upon comparison, it was observed that CT-SLIP differs from PSCU in only two aspects: differences in column cross-sectional dimensions and the location of the beam-end loading. From the experimental results of CT-SLIP, it is noted that the column in CT-SLIP did not undergo plastic deformation throughout the entire test. Simultaneously, during result analysis, the numerical values of beam-end loading were transformed into moments, serving as the indicator for subsequent analyses. Consequently, these two differences do not compromise the validation of the finite element modeling approach. All other model parameters for both types of connections remain identical. The developed FE model of CT-SLIP is depicted in Fig.9.

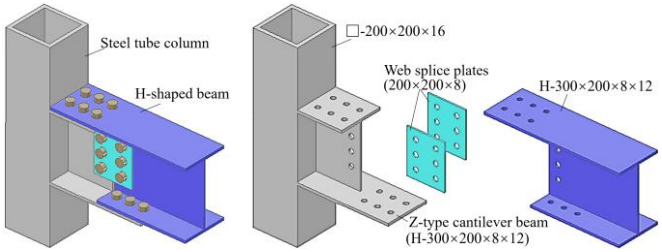

(a) Construction of CT-SLIP (b) Details of CT-SLIP

Fig. 8 The CT-SLIP connection

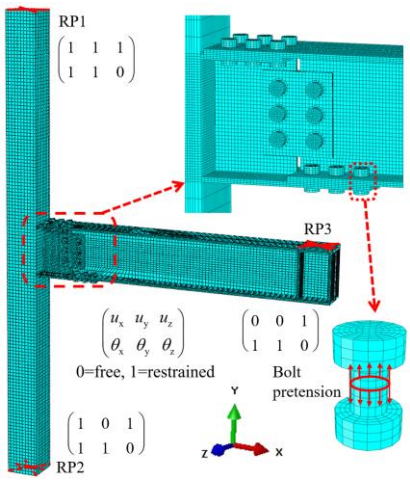

Fig. 9 FE model of CT-SLIP

The low-cycle reciprocating load, which was shown in Fig.7, was applied to the CT-SLIP model, and the finite element results were compared with the experimental results in Reference [30]. As depicted in Fig.10, the failure mode of the CT-SLIP connection obtained through FE analysis is consistent with the experimental failure mode, demonstrating local buckling of the lower flange of the cantilever beam. The stress diagram obtained from the finite element simulation clearly indicate that the stress levels on the cross-section of the column in CT-SLIP consistently remain below the yield strength of the steel. The entire cross-section of the column remains in the elastic phase. This validates the correctness of the earlier assumptions.

Comparing the hysteresis curves from tests and FE analysis reveals that the FE model accurately predicts the ultimate bearing capacity, initial stiffness, and unloading stiffness of CT-SLIP, with only little discrepancies observed in the pinching behavior of the hysteresis curve. This is attributed to the finite element model neglecting initial defects in geometric, material, and contact relationships, along with relatively idealized boundary conditions and uncertainties in material and component properties. As a result, the initial slip moment obtained from the finite element analysis is slightly larger than the experimental value, and the pinching behavior in the finite element curve is slightly less pronounced. Nonetheless, both exhibit a good overall consistency, indicating that the main characteristics of the finite element curve align well with experimental values, affirming the correctness and reliability of the finite element modeling approach adopted in this study.

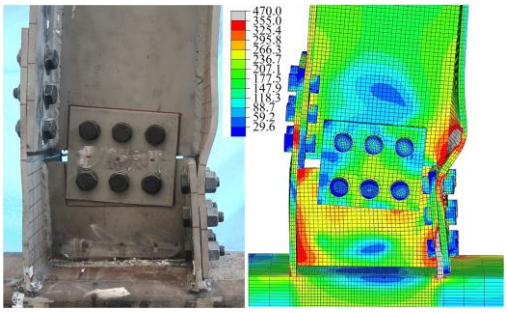

(a) Failure models

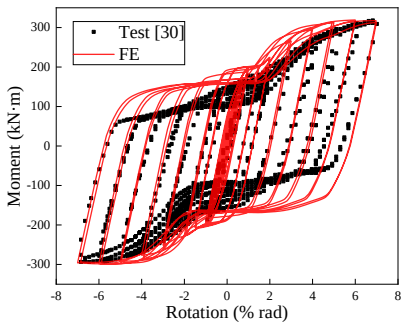

(b) Moment-Rotation curve under cyclic load

Fig. 10 Comparison of test results and FE results for CT-SLIP

4. Numerical analysis of PSCU

4.1. Failure mode of PSCU

The finite element model of PSCU was simulated, and the hysteresis curve and skeleton curve of the connection were extracted, as shown in Fig.11. Stress diagrams of PSCU, relative displacement diagrams of bolt holes, and PEEQ plastic strain diagrams are shown in Fig.12. The analysis reveals the following: 1) When the connection rotation (θ) is less than 0.004rad, both positive and negative skeleton curves exhibit linear variations. The stress in each component of the connection area does not reach the yield strength, and there is no relative slipping, as shown in Fig.12(a) and (b). Thus, it can be defined as: "When $\theta <$ 0.004rad, PSCU is in the elastic stage." 2) When θ reaches 0.004rad, noticeable inflection points appear in both positive and negative skeleton curves, causing a sudden drop in connection stiffness. The stress in each component of the connection area still does not reach the yield strength, but significant relative

slipping occurs between the plates, as shown in Fig.12(c) and (d). Since the slipping stage stops at θ = 0.01rad under positive loading, the bearing capacity of the connection continues to increase. During negative loading, the slipping stage continues until θ = 0.02rad, after which the bearing capacity continues to rise. Thus, it can be defined as: "When 0.004 ≤ θ < 0.01rad (under positive loading) or 0.004 ≤ θ < 0.02rad (under negative loading), PSCU is in the slipping stage." 3) After the slipping stage, the positive and negative load-carrying capacities of the connection significantly increase. At this point, only the maximum stress on the U-shaped plate exceeds its yield strength, and the U-shaped plate starts to yield, as shown in Fig.12(e) and (f). Until θ = 0.04rad, a small yielded area appears at the variable cross-section of the beam end, as shown in Fig.12(g) and (h). In this stage, the maximum bearing capacity of PSCU has not reached its ultimate bearing capacity, but the difference is small. Thus, it can be defined as: "When 0.01 ≤ θ < 0.04 rad (under positive loading) or 0.02 ≤ θ < 0.04 rad (under negative loading), PSCU is in the elastic-plastic stage." 4) With continued loading, the bearing capacity still slightly increases, but the connection rotation significantly increases. Plastic hinges appear at the variable cross-section of the beam end and continue developing. Thus, it can be defined as: "When θ > 0.04 rad, PSCU is in the plastic stage." The loading simulation terminates at θ = 0.07rad due to extremely low efficiency in subsequent calculations.

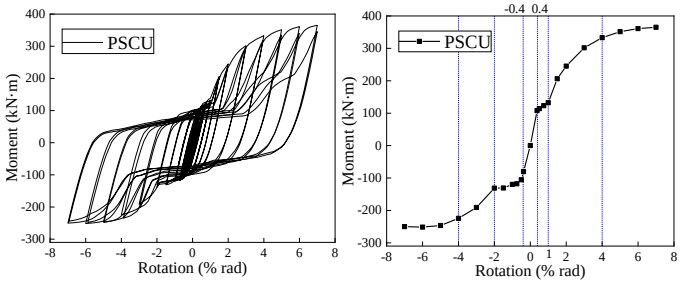

(a) Hysteresis curve (b) Skeleton curve

Fig. 11 FE result curves of PSCU

In light of the foregoing, the entire lateral resistance process of the connection can be delineated into four distinct stages: elastic stage, slipping stage, elastic-plastic stage, and plastic stage, each corresponding to one of the four design criteria depicted in Fig.3. Specifically, under frequent earthquakes, it is imperative for PSCU to maintain an elastic state, with a prescribed inter-story drift angle limit of 0.004rad, a criterion consistent with the stipulations outlined in specifications [31]. In the context of seismic design actions, PSCU is permitted to transition into the slipping stage, wherein none of the constituents within the connection area undergo yield. The connection can exploit frictional energy dissipation, necessitating post-earthquake recovery solely for bolted connections. Under fortification earthquakes, PSCU can harness the yielding behavior of the U-shaped plate for energy dissipation, affording protection to other structural elements. Consequently, the connection enters the elastic-plastic stage, with post-earthquake recovery limited to the U-shaped plate and its corresponding bolted connections. The inter-story drift angle limit at this juncture is set at 0.04, manifesting a conspicuous surplus in contrast to the elastic-plastic inter-story drift angle limit delineated in specifications [31]. In instances of extremely rare earthquakes, the plastic hinge can be formed at the variable cross-section of the frame beam, thereby augmenting the structural capacity for energy dissipation. Subsequent to seismic occurrences, restorative measures might necessitate the replacement of the beam. These deductions substantiate the accuracy of the seismic design objectives and post-earthquake recovery methodologies expounded in Section 2.2 of this discourse.

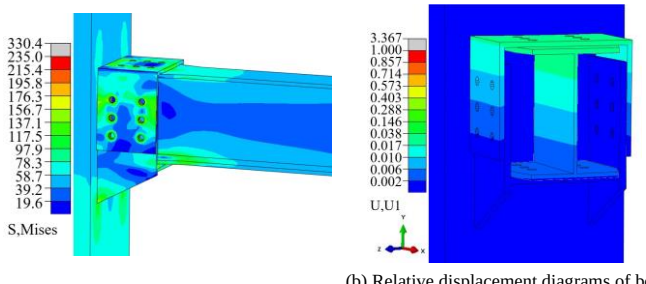

(a) Stress diagrams (θ=0.004rad) (b) Relative displacement diagrams of bolt holes (θ=0.004rad)

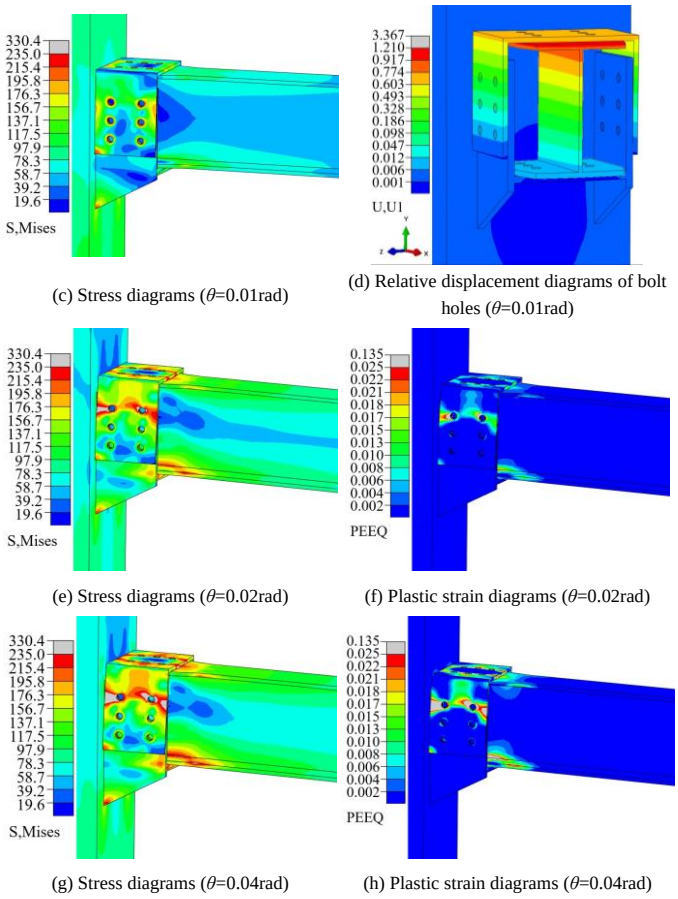

(c) Stress diagrams (θ=0.01rad) (d) Relative displacement diagrams of bolt holes (θ=0.01rad)

(e) Stress diagrams (θ=0.02rad) (f) Plastic strain diagrams (θ=0.02rad)

(g) Stress diagrams (θ=0.04rad) (h) Plastic strain diagrams (θ=0.04rad)

Fig. 12 FE result diagrams of PSCU

4.2. Seismic performance evaluation of PSCU

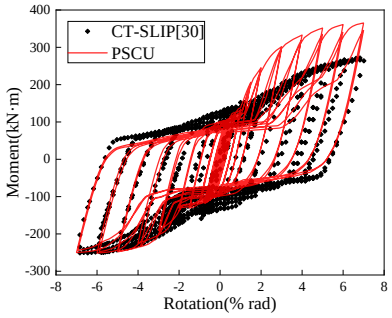

Fig. 13 Comparison of the hysteretic curves between PSCU and CT-SLIP

Comparing the key performance indicators of PSCU and CT-SLIP as presented in Table 3 reveals that the two models differ only in the construction at the connection area. Analyzing the hysteresis curves of both models provides an effective preliminary assessment of the seismic performance of PSCU. A comparison of the hysteresis curves of PSCU and CT-SLIP, as shown in Fig. 13, yields the following insights:

1) The hysteresis curve of PSCU exhibits asymmetry in both positive and negative directions, attributed to the structural asymmetry of the upper and lower parts of the connection area of PSCU. Under positive loading conditions, the PSCU undergoes slipping, culminating in the top of the U-shaped plate making contact with the column. Subsequently, a substantial portion of anticlockwise bending moment is directly transmitted to the column through the U-shaped plate. Under negative loading, the PSCU has limited bending moment transmission capacity, as only the bottom corners of the U-shaped plate contact the column after slipping. Additionally, the longer duration of slipping under negative loading results in a noticeably smaller negative ultimate bearing capacity compared to the positive one.

2) The more pronounced pinching effect in the hysteresis curve of PSCU indicates a smaller residual displacement after seismic shaking compared to CT-SLIP. This is advantageous for the post-earthquake recoverability of the connection.

Table 3 provides the key performance indicators for PSCU and CT-SLIP.

Among them, the ultimate moment (M_u) represents the moment corresponding to the maximum rotation (θ_u), and the ductility coefficient (μ) is the ratio of the maximum rotation to the slipping rotation (θ_s) [30]. Due to the absence of a significant reduction in load-bearing capacity throughout the loading process, the actual ductility coefficient of PSCU should be greater than the calculated value in the table. A comparison with CT-SLIP reveals that under positive loading, PSCU exhibits a significantly higher initial stiffness (K_0), and under negative loading, its initial stiffness is comparable to that of CT-SLIP. PSCU has a smaller slipping moment, indicating a greater tendency for relative slipping between its components. Moreover, PSCU demonstrates higher ultimate bearing capacity, superior ductility, and comparable energy dissipation capacity (E) to CT-SLIP.

Table 3
Key performance indicators of CT-SLIP and PSCU

Connection	Direction	K_0 (kN/mm)	θ_s (% rad)	M_s (kN·m)	θ_u (% rad)	M_u (kN·m)	μ	E (kJ)
CT-SLIP	Positive	5.65	0.74	149.75	6.88	277.41	9.33	249.02
	Negative	5.76	0.73	152.65	6.85	252.64	9.32	
PSCU	Positive	7.56	0.43	107.79	7.00	365.15	>16.27	252.39
	Negative	5.62	0.50	105.44	6.01	251.46	>12.02	

Combining the analysis of the failure mode of PSCU, it is evident that PSCU not only effectively fulfills the initial seismic design objectives, meeting current standards, but also enhances the ultimate bearing capacity, ductility, and post-earthquake repairability of prefabricated steel frame beam-column connections while ensuring overall energy dissipation performance.

5. Parametric analysis of PSCU

Utilizing the PSCU as the foundational model (BASE), this study systematically examines the influence patterns of distinct parameters on the seismic resistance and post-earthquake functional recovery of this connection. The investigated parameters encompass variations in the U-shaped plate thickness (t_U), T-shaped plate thickness (t_T) and the quantity of connecting bolts in different orientations. Model designations and their respective parameter metrics are delineated in Table 4.

Table 4
Parameters of FE models

Model	t_U (mm)	t_T (mm)	n_u	n_s	n_b
BASE	12	16	6	6	6
U-10	10	16	6	6	6
U-16	16	16	6	6	6
T-12	12	12	6	6	6
T-18	12	18	6	6	6
TP-4	12	16	4	6	6
TP-8	12	16	8	6	6
WB-4	12	16	6	4	6
WB-8	12	16	6	8	6
BT-4	12	16	6	6	4
BT-8	12	16	6	6	8

Notes: n_u, n_s and n_b are the number of the upper flange bolts, number of bolts on one side and number of the lower flange bolts, respectively.

5.1. U-shaped plate thickness

Through finite element analysis and theoretical calculations on the 11 models presented in Table 4, key performance indicators for each model were obtained, as detailed in Table 5. Failure modes, hysteresis curves, and skeleton curves were extracted for the U-10, BASE, and U-16 models, as illustrated in Fig.14. Comparative analysis of the finite element simulation results for these three models reveals the following:

1) As the thickness of the U-shaped plate increases, the stress at both the T-shaped plate and the beam end significantly increases. When the U-plate thickness is 16mm, in the final loading stage, certain regions of the T-shaped plate also undergo plastic deformation, which contradicts the post-earthquake functional recovery requirement;

2) The increase of U-shaped plate thickness has a negligible impact on the initial stiffness (K_0) and slipping moment (M_s) of PSCU, with no significant effect on the slipping angle (θ_s);

3) The ultimate bearing capacity (M_u) of the connection correlates positively with the increase in U-shaped plate thickness, especially in the negative direction of connection bearing capacity. Enlarging U-shaped plate thickness significantly diminishes the discrepancy in positive and negative ultimate bearing capacities of PSCU.

4) A comparative analysis of finite element results and theoretical results indicates an error margin generally within 7%, with theoretical results consistently undershooting finite element results. This underscores the scientific and accurate nature of the theoretical model established in Section 2.2.

Table 5
Key performance indicators of FE models

Model	Direction	K_0 (kN/mm)	θ_s (% rad)	M_s (kN·m)	θ_u (% rad)	M_u (kN·m)	μ	E (kJ)	$M_{s,t}$ (kN·m)	$M_{u,t}$ (kN·m)
BASE	Positive	7.56	0.43	107.79	7.00	365.15	>18.7	204.4	102.5	360.7
	Negative	5.62	0.50	105.44	6.01	251.46	>12.0		100.6	238.8
U-10	P	7.49	0.42	106.83	6.99	357.69	>18.7	189.2	101.9	355.3
	N	5.45	0.50	102.68	5.02	214.54	>10.0		100.3	199.6
U-16	P	7.69	0.42	109.65	7.01	378.07	>18.7	225.0	102.9	370.2
	N	5.88	0.50	108.87	7.00	318.59	>14.0		100.9	308.4
T-12	P	6.69	0.43	95.33	7.00	324.99	>18.7	175.3	100.6	336.3
	N	5.64	0.50	103.31	7.00	247.36	>14.0		99.1	238.8
T-18	P	7.91	0.44	112.34	7.00	365.28	>18.7	210.6	103.8	369.1
	N	6.03	0.50	109.08	6.02	258.46	>12.0		102.8	238.8
TP-4	P	7.45	0.41	106.28	7.00	361.40	>18.7	194.7	102.5	360.7
	N	5.49	0.44	78.32	5.03	249.64	>13.3		84.8	238.8
TP-8	P	7.57	0.42	107.94	7.00	370.21	>18.7	195.5	102.5	360.7
	N	5.54	0.50	72.02	6.00	245.31	>16.0		80.5	238.8
WB-4	P	7.48	0.43	106.62	6.99	363.54	>18.7	183.4	102.5	360.7
	N	4.99	0.42	68.09	7.02	245.94	>18.7		67.1	216.9
WB-8	P	7.57	0.44	107.82	6.02	363.15	>16.0	220.8	102.5	360.7
	N	5.94	0.50	113.62	6.00	262.92	>12.0		119.2	272.6
BT-4	P	5.60	0.42	79.82	6.01	327.80	>18.7	187.4	74.6	300.6
	N	5.56	0.50	102.26	7.01	248.95	>14.0		100.6	238.8
BT-8	P	8.71	0.44	124.21	7.03	397.13	>18.7	221.2	122.7	412.3
	N	5.72	0.50	106.98	6.02	260.21	>12.0		100.6	238.8

Notes: $M_{s,t}$ and $M_{u,t}$ are the theoretical results of slip moment and ultimate moment, respectively, which were calculated by Eq.(1)-(3).

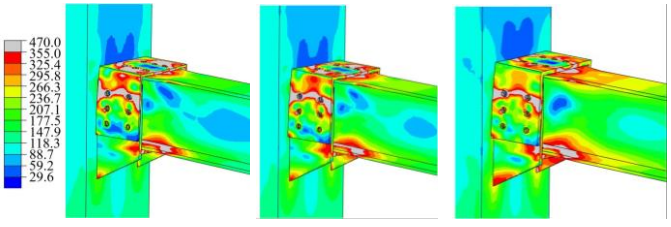

(a) U-10 (b) BASE (c) U-16

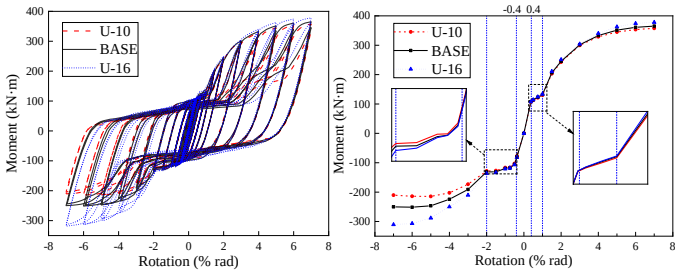

(d) Hysteretic curves (e) Skeleton curves

Fig. 14 Failure modes and result curves of FE models

5.2. T-shaped plate thickness

The failure modes, hysteresis curves, and skeleton curves of the models of T-12, BASE, and T-18 are extracted, as shown in Fig.15. Combining the key performance indicators of these 3 models in Table 5, the analysis indicates that:

1) As the thickness of the T-shaped plate increases, the stress within the plate decreases markedly, the yielding zone in the U-shaped plate remains essentially unchanged, and there is a slight decrease in stress at the variable cross-section of the beam end;

2) When the thickness of the T-shaped plate is 12mm, PSCU only exhibits a significant decrease in slip load and ultimate bearing capacity under positive loading, with the initial stiffness of the overall connection decreasing by 12% compared to the BASE model, and a 14.2% decrease in cumulative energy dissipation. This indicates that in the design of PSCU, priority should be given to ensuring that the T-shaped plate does not yield, thereby ensuring that the connection has good seismic performance, which is also an important condition for achieving the post-earthquake functional recovery of PSCU;

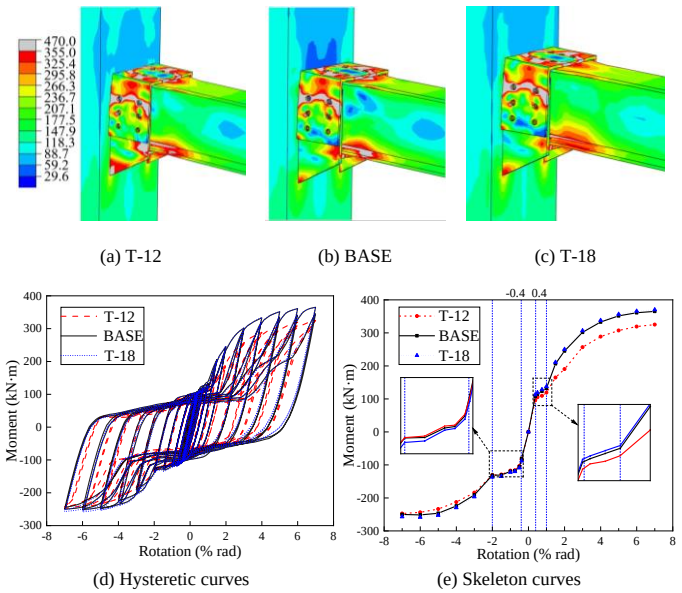

(a) T-12 (b) BASE (c) T-18

(d) Hysteretic curves (e) Skeleton curves

Fig. 15 Failure modes and result curves of FE models

3) When the thickness of the T-shaped plate is 18mm, PSCU only has a slight increase in initial stiffness (4.6% increase in positive direction, 7.3% increase in negative direction), and the improvement in other performance indicators does not exceed 3%. This indicates that once the T-shaped plate does not yield during loading, increasing its thickness does not significantly affect the seismic performance of the PSCU;

4) The error between the finite element results and the theoretical results can still be controlled within 10%, indicating that the accuracy of the theoretical model can still be ensured after changing the thickness of the T-shaped plate.

5.3. Number of bolts connecting between U-shaped plate and upper flange of beam

The failure modes, hysteresis curves, and skeleton curves of the models of TP-4, BASE, and TP-8 are extracted, as shown in Fig.16. Combining the key performance indicators of these 3 models in Table 5, the analysis indicates that:

1) The number of connecting bolts on the upper flange of the beam has a negligible impact on the initial stiffness and ultimate bearing capacity of the PSCU;

2) Reducing the number of connecting bolts on the beam upper flange has a minor effect on the load-bearing capacity of the PSCU under positive loading conditions, but it significantly influences the negative slipping process. This occurs because a reduction in the number of connecting bolts decreases the maximum static friction between the U-shaped plate and the beam upper flange. When the external load reaches this maximum static friction force, the U-shaped plate slides first between the upper flange of the beam until the bolt rod contacts the hole wall, and then the remaining bolt connections begin to slide, forming a two-stage slipping phenomenon, as shown by the red curve in Fig.16 (e);

3) Increasing the number of connecting bolts on the upper flange of the beam only does not enhance the slipping load of the PSCU. This is because while adding more bolts significantly raises the maximum static friction force between the U-shaped plate and the beam upper flange, it also makes sliding at that specific connection more difficult. Consequently, other bolt connections may experience premature slipping, resulting in minimal overall slipping of the beam upper flange throughout the loading process;

4) Comparing the cumulative energy dissipation, it can be obtained that regardless of whether the number of bolts is increased or decreased, the cumulative energy dissipation of the connection is reduced (compared to the BASE model, TP-4 is reduced by 4.7%, and TP-8 is reduced by 4.4%), indicating that appropriate slipping between the components contributes to the energy dissipation of PSCU.

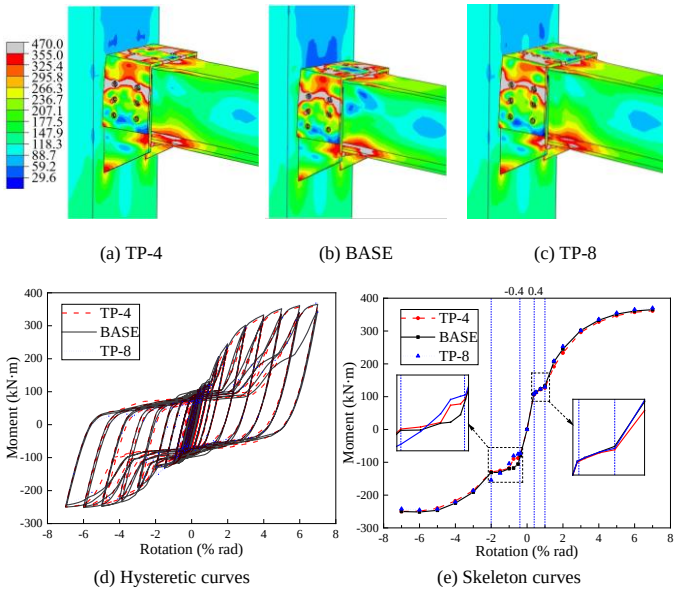

(a) TP-4 (b) BASE (c) TP-8

(d) Hysteretic curves (e) Skeleton curves

Fig. 16 Failure modes and result curves of FE models

5.4. Number of bolts connecting between U-shaped plate and T-shaped plate on one side

The failure modes, hysteresis curves, and skeleton curves of the models of WB-4, BASE, and WB-8 are extracted, as shown in Fig.17. Combining the key performance indicators of these 3 models in Table 5, the analysis indicates that:

1) The influence of increasing the number of bolts connecting the U-shaped plate and T-shaped plate on the ultimate bearing capacity, initial stiffness, and positive slip load of PSCU remains inconspicuous;

2) The reduction in the number of bolts connecting the U-shaped plate and T-shaped plate has a significant impact on the negative slipping process of PSCU. This occurs because a reduction in the number of bolts connecting the U-shaped plate and the T-shaped plate directly results in a decrease in the maximum static friction force between the two components. When the external load reaches this maximum static friction force, slip occurs first between the U-shaped plate and the T-shaped plate, until the bolt shank contacts the hole wall at this point, after which the remaining bolted connections start to slip, thereby forming a two-stage slip phenomenon, as shown by the red curve in Fig.17(e);

3) Only increasing the number of bolts connecting the U-shaped plate and T-shaped plate can increase the negative slip load of PSCU, but its effect is minimal. The sequence of slipping is characterized by the initial slipping of the bolted connections at the upper and lower flanges of the beam, followed by the subsequent slipping of the bolted connections between the U-shaped plate and the T-shaped plate. This results in a two-stage slip phenomenon, as illustrated by the blue curve in Fig. 17(e);

4) Comparing the cumulative energy dissipation, it can be seen that the cumulative energy dissipation of the connection is increased with the increasing

of the number of bolts (compared to the BASE model, WB-4 is reduced by 10.3%, and WB-8 is increased by 8.1%). An observation of the hysteresis curve in Fig. 17(d) reveals that the hysteresis curve for WB-4 exhibits significant pinching. This phenomenon is attributable to the relatively small number of bolts connecting the U-shaped plate and the T-shaped plate in WB-4. With the increase of cyclic loading, the loss of bolt pre-tension force and friction coefficient is severe, and the slip energy dissipation mechanism basically disappears. Therefore, ensuring the reliability of the bolted connection between the U-shaped plate and T-shaped plate is beneficial for improving the energy dissipation performance of PSCU.

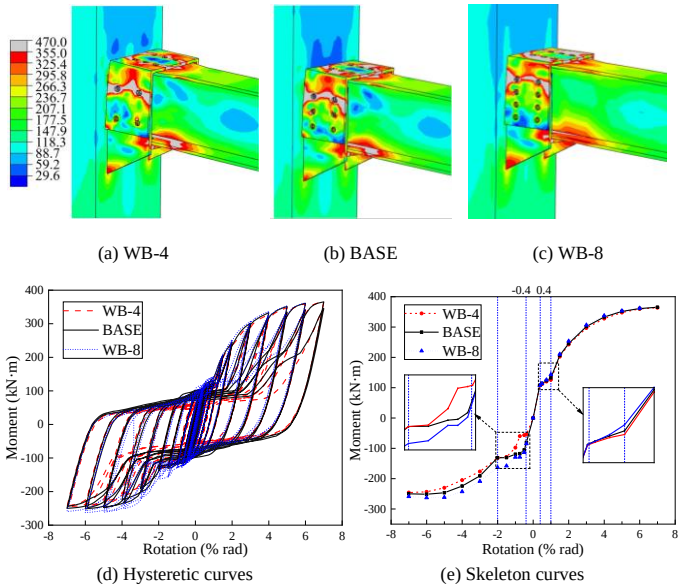

(a) WB-4 (b) BASE (c) WB-8

(d) Hysteretic curves (e) Skeleton curves

Fig. 17 Failure modes and result curves of FE models

5.5. Number of bolts connecting between T-shaped plate and lower flange of beam

The failure modes, hysteresis curves, and skeleton curves of the models of BT-4, BASE, and BT-8 are extracted, as shown in Fig.18. Combining the key performance indicators of these 3 models in Table 5, the analysis indicates that:

1) As the number of connecting bolts between the lower flange of the beam increases, the stress on both the T-shaped plate and the variable cross-section at the beam end rises significantly, and the T-shaped plate of BT-8 has already yielded after loading, which does not meet the requirement for the post-earthquake functional recovery of PSCU;

2) Increasing the number of connecting bolts in the lower flange of the beam has little influence on the negative ultimate bearing capacity, negative initial stiffness, and negative slip load of PSCU;

3) Strengthening the connection strength of the lower flange of the beam will significantly increase the positive stiffness and slip load of PSCU, and at the same time, the positive ultimate bearing capacity of PSCU will also be significantly improved, but this will also make the difference in positive and negative bearing capacities of PSCU more apparent;

4) The cumulative energy dissipation capacity of PSCU significantly improves with the increase in the number of connecting bolts in the lower flange of the beam. This enhancement is attributed not only to the improved positive bearing capacity but also to the reduction in hysteresis curve pinching, which is effectively mitigated by the greater number of bolts.

Considering the analysis results of Sections 5.3, 5.4, and 5.5, and taking into account the seismic performance and the requirement for post-earthquake functional recovery of PSCU, the following design recommendations can be made: To prevent yielding of the T-shaped plate, it is recommended that the number of connecting bolts on the upper flange, lower flange of the beam, and between the U-shaped plate and the T-shaped plate on each side should be kept consistent.

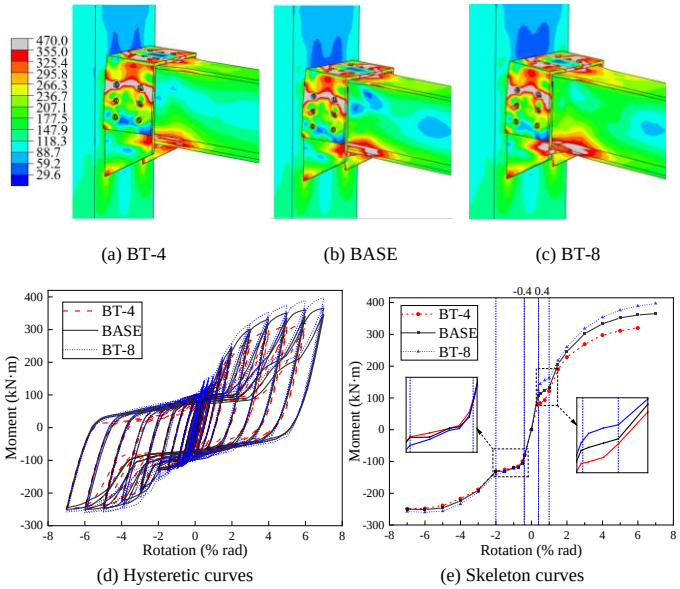

(a) BT-4 (b) BASE (c) BT-8

(d) Hysteretic curves (e) Skeleton curves

Fig. 18 Failure modes and result curves of FE models

6. Conclusion

To investigate the seismic performance and post-earthquake recovery of PSCU, this study employed theoretical methods to establish design criteria and post-earthquake recovery methods for PSCU, and derived design equations for PSCU. Additionally, a refined finite element (FE) model of PSCU was developed and validated, and parameterized numerical analysis of PSCU was conducted. The main conclusions are as follows:

(1) The failure mode of PSCU belongs to typical ductile failure, and even when the rotation angle reaches 0.07rad, PSCU can still ensure the integrity of non-replaceable components, thereby ensuring its good post-earthquake recovery performance.

(2) The entire lateral resistance process of PSCU can be delineated into four distinct stages: elastic stage (the connection rotation angle θ < 0.004rad), slipping stage ($0.004 \le \theta < 0.01$rad under positive loading or $0.004 \le \theta < 0.02$rad under negative loading), elastic-plastic stage ($0.01 \le \theta < 0.04$ rad under positive loading or $0.02 \le \theta < 0.04$ rad under negative loading), and plastic stage ($\theta >$ 0.04 rad).

(3) PSCU can meet the post-earthquake functional recovery requirements through the following measures, namely “no repair is needed in the elastic stage, only bolted connection repair is needed in the slip stage, only U-shaped plate replacement is needed in the elastic-plastic stage, and U-shaped plate and beam replacements are needed in the plastic stage”.

(4) When designing PSCU, the thickness of the U-shaped plate should not exceed that of the T-shaped plate to ensure that the T-shaped plate does not yield throughout the entire lateral resistance process. Bolted connections can be designed based on the elastic limit of the PSCU, and the number of bolts on each connected surface should be as uniform as possible.

(5) By comparing the finite element (FE) results with the theoretical results of all models, it can be obtained that the maximum error is 12%, with an average error of less than 3%. The high level of agreement between the FE results and the theoretical results indicates that theoretical design equations of PSCU established in this paper is relatively scientific and accurate.

Acknowledgement

This research was funded by the Key Research and Promotion Project (Scientific and Technological Project) of Henan Province (No. 242102321013), Postdoctoral research grant in Henan Province (No. 202103010), China Postdoctoral Science Foundation (No. 2023M733248), Scientific and Technological Innovation Leaders in Central Plains of Henan Province (No. 234200510022), and the Support Program for Innovative Research Team (in Science and Technology) in University of Henan Province (No. 23IRTSTHN006).

References

[1] X.C. Liu, S.H. Pu, A.L. Zhang, et al, Performance analysis and design of bolted connections in modularized prefabricated steel structures, Journal of Constructional Steel Research, 2017, 133, 360-373.

[2] Zhang A L, Shangguan G H, Zhang Y X, et al. Experimental study of resilient prefabricated steel frame with all-bolted beam-to-column connections. Advanced Steel Construction, 2020,

16(3): 255-271.
[3] K. Oh, R. Li, L.Y. Chen, et al, Cyclic Testing of steel column-tree moment connections with weakened beam splices, International Journal of Steel Structures, 2014, 14, 471-478.
[4] Koken A, Hatipoglu E T. Investigation of the behavior of weakened and strengthened steel column-beam connections under seismic effects. Advanced Steel Construction, 2014, 10: 1-13.
[5] Guo Y, Yao X. Seismic performance and design of reduced steel beam section with concrete filled square tubular column. Advanced Steel Construction, 2013, 9(3): 173-189.
[6] X.H. Zhang, S.S. Zheng, X.R. Zhao, Seismic performance of steel beam-to-column moment connections with different structural forms, Journal of Constructional Steel Research, 2019, 158, 130-142.
[7] H.B. Liu, J. Lan, Z.H. Chen, et al, Study on the seismic behavior of connection via welding strengthening under load, Journal of Constructional Steel Research, 2022, 196, 107387.
[8] Y.Z. Tian, M. Liu, Z.H. Jia, et al, Study on mechanical behavior and optimization of prefabricated square column H-beam outer-shell joint, Mechanics of Advanced Materials and Structures, 2019, 19, 1-8.
[9] X.C. Liu, X.X. Zhan, S.H. Pu, et al, Seismic performance study on slipping bolted truss-to-column connections in modularized prefabricated steel structures, Engineering Structures, 2018, 163, 241-254.
[10] X.L. Lv, Y. Chen, Y.J. Mao, New concept of structural seismic design: earthquake resilient structures, J Tongji Univ, 2011, 39, 941-948(in Chinese).
[11] X.L. Lv, Y. Chen, H.J. Jiang, Research progress in structural systems with replaceable members, Earthquake Engineering Structural Dynamics, 2014, 34, 27-36 (in Chinese).
[12] Zhao L Y, Guo D, Yang Y Q, et al.Seismic Performance and Replaceability of Steel Frame Structures with Replaceable Beam Segments. Advanced Steel Construction,2024, 20(1): 69-80.
[13] Zhang Y, Wang Z, Zhao W, et al. A pseudo-dynamic test study on a self-centering prefabricated steel frame with a column base connected by semi-rigid joints. Advanced Steel Construction, 2016, 12(3): 296-315.
[14] Y.Z. Chen, L.W. Tong, Y.Y. Chen, Experimental study on cyclic behavior of cast steel connectors for beam-to-column joints, Journal of Structural Engineering, 2016, 19, 1677-1695.
[15] M. Rui, L. Válter, P. Stefano, Development of steel angles as energy dissipation devices for rocking connections, Structural Concrete, 2018, 25, 1-15.
[16] M. Wang, P. Bi, Study on seismic behavior and design method of dissipative bolted joint for steel frame with replaceable low yield point steel connected components, Construction and Building Materials, 2019, 198, 677-695.
[17] M. Wang, X.G. Ke, Seismic design of widening flange connection with fuses based on energy dissipation, Journal of Constructional Steel Research, 2020, 170, 106076.
[18] A.L. Zhang, Q. Wang, Z.Q. Jiang, et al, Experimental study of earthquake-resilient prefabricated steel beam-column joints with different connection forms, Engineering Structures, 2019, 187, 299-313.
[19] Z.Q. Jiang, X.F. Yang, C. Dou, et al, Cyclic testing of replaceable damper: earthquake-resilient prefabricated column-flange beam-column joint, Engineering Structures, 2019, 183, 922-936.
[20] Z.Q. Jiang, T. Lan, C. Dou, et al, Cyclic loading tests of earthquake-resilient prefabricated cross joint with single flange cover plate, Journal of Constructional Steel Research, 2020, 164, 105752.
[21] Z.Q. Jiang, S.H. Lin, X.C. Liu, et al, Influence of bolts on seismic performance of earthquake-resilient prefabricated sinusoidal corrugated web steel beam-column joints, Journal of Constructional Steel Research, 2020, 172, 106214.
[22] A.L. Zhang, H. Zhang, Z.Q. Jiang, et al, Low cycle reciprocating tests of earthquake-resilient prefabricated column-flange beam-column joints with different connection forms, Journal of Constructional Steel Research, 2020, 164, 105771.
[23] Z.Q. Jiang, C. Dou, H. Zhang, et al, Experimental study of earthquake-resilient prefabricated beam-column steel joint with L-shaped plate, Journal of Constructional Steel Research, 2020, 166, 105928.
[24] Z.Q. Jiang, Z.Y. Niu, K.K. Cheng, et al, Experimental study of earthquake-resilient high ductility prefabricated opening-web steel channel beam-column joint, Journal of Building Engineering, 2022, 49, 104041.
[25] Z.X. Bai, C.J. Shen, Z.Q. Jiang, et al, Cyclic loading tests of an earthquake-resilient prefabricated steel frame with open-web steel channel beams, Journal of Constructional Steel Research, 2021, 177, 106477.
[26] X.W. Zhang, X. Rong, X.N. Shi, et al, Experimental evaluation on the seismic performance of high-strength reinforcement beam-column joints with different parameters, Structures, 2023, 51, 1591-1608.
[27] ANSI/AISC 341-16. Seismic Provisions for Structural Steel Buildings. Chicago, USA, American Institute of Steel Construction, 2016.
[28] A.L. Zhang, Z.P. Guo, X.C. Liu, Seismic performance of Z-type cantilever beam splices of column–tree connection, Journal of Constructional Steel Research, 2017, 133, 97-111.
[29] Z.P. Guo, A.L. Zhang, X.C. Liu, et al, Seismic behavior of prefabricated steel frame connection with Z-shaped cantilever beam and reduced beam section, Journal of Building Structures, 2017, 38, 43-52 (in Chinese).
[30] A.L. Zhang, Z.P. Guo, X.C. Liu, et al, Experimental study on seismic performance of prefabricated steel frame joints with Z-shaped cantilever beam segment splicing, Engineering Mechanics, 2017, 34, 31-41(in Chinese).
[31] GB50017-2017. Code for Design of Steel Structures. Beijing, China, 2017.Chan S.L. and Chui P.T., Non-Linear Static and Cyclic Analysis of Steel Frames with Semi-Rigid Connections, Elsevier, New York, 2000.